



Magnetic mineralogy of the Yaxcopoil-1 core, Chicxulub

Mark PILKINGTON,^{1*} Doreen E. AMES,¹ and Alan R. HILDEBRAND²

¹Geological Survey of Canada, 615 Booth Street, Ottawa, Ontario K1A 0E9, Canada

²Department of Geology and Geophysics, University of Calgary, 2500 University Drive NW, Calgary, AB, T2N 1N4, Canada

*Corresponding author. E-mail: mpilking@nrcan.gc.ca

(Received 5 September 2003; revision accepted 29 April 2004)

Abstract—Core from the Yaxcopoil-1 (Yax-1) hole, drilled as a result of the Chicxulub Scientific Drilling Project (CSDP), has been analyzed to investigate the relationship between opaque mineralogy and rock magnetic properties. Twenty one samples of suevite recovered from the depth range 818–894 m are generally paramagnetic, with an average susceptibility of 2000×10^{-6} SI and have weak remanent magnetization intensities (average 0.1 A/m). The predominant magnetic phase is secondary magnetite formed as a result of low temperature (<150 °C) alteration. It occurs in a variety of forms, including vesicle infillings associated with quartz and clay minerals and fine aggregates between plagioclase/diopside laths in the melt. Exceptional magnetic properties are found in a basement clast (metamorphosed quartz gabbro), which has a susceptibility of $>45000 \times 10^{-6}$ SI and a remanent magnetization of 77.5 A/m. Magnetic mafic basement clasts are a common component in the Yax-1 impactite sequence. The high susceptibility and remanence in the mafic basement clasts are caused by the replacement of amphiboles and pyroxenes by an assemblage with fine <1 µm magnetite, ilmenite, K-feldspar, and stilpnomelane. Replacement of the mafic minerals by the magnetic alteration assemblage occurred before impact. Similar alteration mechanisms, if operative within the melt sheet, could explain the presence of the high amplitude magnetic anomalies observed at Chicxulub.

INTRODUCTION

Magnetic data collected over the Chicxulub impact structure (Fig. 1) have been crucial in its discovery and exploration. A 1978 aeromagnetic survey of the northwestern part of the Yucatán peninsula delineated a circular zone of high amplitude anomalies, which was suggested to be caused by a large buried impact crater (Penfield and Camargo 1981). Subsequent to the establishment of Chicxulub as the K/T boundary crater (Hildebrand et al. 1991; Sharpton et al. 1992), interpretation of magnetic data has provided useful constraints on defining the crater morphology (Pilkington et al. 1994; Espindola et al. 1995; Pilkington and Hildebrand 2000; Rebolledo-Vieyra 2001). Modeling of the magnetic field over Chicxulub is greatly simplified since magnetization contrasts of three to four orders of magnitude exist between the target rocks and several of the impact lithologies. Hence, different structural elements of the crater can be isolated and modeled based on their magnetic properties.

Magnetic anomalies related to the Chicxulub structure can be divided into three concentric zones with a center coincident with that indicated by the gravity anomalies (Penfield and Camargo 1981). The innermost zone consists of

a 20 km radius, simply-shaped, high amplitude (>500 nT) anomaly, interpreted as due to the central uplift. The intermediate zone comprises numerous, large amplitude (hundreds of nT), short wavelength, dipolar anomalies out to a 45 km radius, likely caused by sources within the crater's melt sheet. The outer zone extends out to ~80 km radius and consists of a number of low amplitude (<50 nT), short-wavelength anomalies probably related to ejected material (impact melt/breccia).

Magnetic anomaly modeling at Chicxulub has been constrained by available rock property measurements of impact and target lithologies. These are, however, limited to drill core samples from the Yucatán-6 (Y-6) and UNAM-5,6 and 7 holes. Impact melt rock from Y-6, located within the crater, gives remanent magnetizations of 0.08–0.60 A/m (Sharpton et al. 1992; Steiner 1996), while melt breccia has values of 0.12–0.35 A/m (Urrutia-Fucugauchi et al. 1994). On the basis of magnetic susceptibility, ejecta breccia from UNAM-7 was divided into an upper unit with predominantly basement clasts and an average susceptibility of 55×10^{-6} SI and a lower unit comprising mainly evaporite clasts with values of $<5 \times 10^{-6}$ SI (Urrutia-Fucugauchi et al. 1996a, b). UNAM-6 and UNAM-5 show similar values for the lower

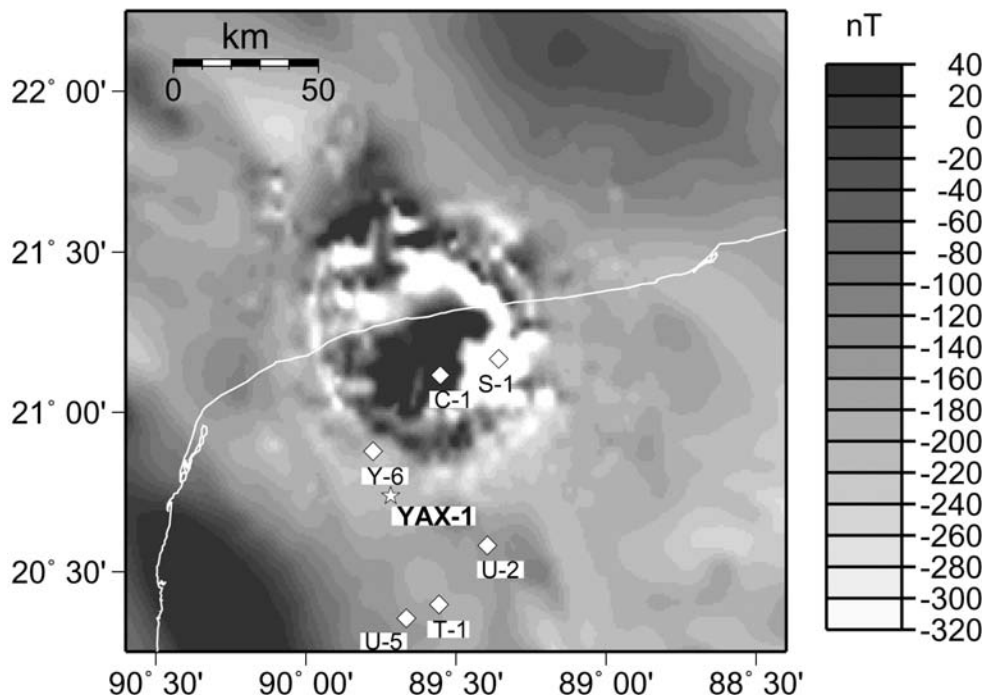


Fig. 1. Magnetic field over Chicxulub with drillhole locations.

and upper breccia units, respectively (Rebolledo-Vieyra 2001). The overlying Tertiary carbonates and evaporites are distinguished by very low susceptibilities ranging -1 to 0×10^{-6} SI (Urrutia-Fucugauchi et al. 1996a, b). Underlying Cretaceous carbonates and evaporites have similar properties; they are also essentially non-magnetic (Hildebrand et al. 1991). Little is known about the magnetic properties or even the lithologies that make up the crystalline basement in the Yucatán peninsula (Lopez-Ramos 1975). Long wavelength (>50 km) magnetic anomalies with amplitudes of several hundred nanoteslas indicate appreciable magnetization contrasts (several A/m) in the basement rocks assuming they have a depth of 4–5 km. Based on the differences in ejecta and basement clast compositions as a function of location, some lithological variation in the basement is undoubtedly present (Sharpton et al. 1992).

The magnetization levels measured so far for impact melt rocks, melt, and ejecta breccia are not sufficient to produce the high amplitude anomalies observed within the two innermost concentric zones, i.e., anomalies thought to be sourced in the central uplift and melt sheet. Based on modeling, these anomalies require magnetizations of ~ 5 A/m (Pilkington et al. 1994; Espindola et al. 1995) compared to average measured values at least ten times smaller. Hence, a mechanism is required to produce such elevated magnetization levels. From the inversion of magnetic field data processed to isolate anomalies from only shallow (presumably melt sheet) sources, Pilkington and Hildebrand (2000) showed that two concentric zones of enhanced magnetization exist at Chicxulub. The inner zone, with a radius of ~ 20 km, coincides with the edge

of the central uplift, while the outer zone at ~ 45 km radius occurs at the edge of the transient cavity. These zones were interpreted to be caused by the result of an impact-generated hydrothermal system with alteration controlled by fracture zones and paleotopographic highs (i.e., central uplift). Radial and concentric fracture distributions within melt sheets are characteristic of large impact structures (Alexopoulos and McKinnon 1994). For Chicxulub these would be expected to exist out to a radius of ~ 45 km. The character of the magnetic anomalies associated with the two concentric zones indicates that the causative magnetization has a reversed polarity, which suggests that the hydrothermal systems were active within the same geomagnetic polarity interval (chron 29r) as at the time of impact and that the anomalies are produced by magnetic phases with a predominantly remanent magnetization component. Although the location, approximate geometry, and magnetization strength of these alteration zones are well-constrained by the magnetic field data, the nature of the magnetic phases and their origin are, as yet, unknown. In this paper, petrographic and rock magnetic studies of the Yaxcopoil-1 (Yax-1) drill core are carried out to determine direct constraints on the source of the magnetic anomalies observed at Chicxulub.

YAX-1 DRILLHOLE

The Yax-1 hole was drilled as a result of the CSDP under the auspices of the International Continental Drilling Program (ICDP). The hole bottoms at 1511 m and core from 404–1511 m was recovered. Yax-1 is located at 20.740°N

89.718°W, approximately 16 km south-southeast of the Y-6 drillhole (Fig. 1). In terms of crater structure, as defined by geophysical data, Yax-1 is placed outside the transient cavity, within the zone of slumped blocks. Hence, Yax-1 is outside the intermediate magnetic zone of high amplitude anomalies probably related to hydrothermal alteration controlled by fracture systems, paleotopographic highs in the basement (central uplift) and the edge of the melt sheet. Yax-1 is located in the (outermost) magnetic zone of low amplitude (<50 nT) anomalies most likely associated with ejected material. Gravity data show that Yax-1 is positioned roughly half-way between two concentric lines of horizontal gravity gradient maxima, which are thought to indicate the edges of individual slumped blocks within the megaterrace zone (Hildebrand et al. 1995). The Yax-1 core, starting at 404 m, consists of Tertiary platform carbonates down to the K/T boundary at 794 m. Below this is a series of impact melt-rich suevites and breccias down to 895 m, which has been divided into six units (Dressler et al. 2003; Stöffler et al. 2003). These are underlain by displaced carbonates and anhydrite with minor breccia dykes, representative of the megablock zone, and finally, Cretaceous carbonate rocks.

MAGNETIC MEASUREMENTS

Susceptibilities of 21 samples from the depth interval of 818–894 m were measured on a Sapphire Instruments SI-2b low-field magnetic susceptibility meter. Samples were cut from the core to produce pieces with volumes ranging from 3.7 to 7.7 cm³. The samples are paramagnetic with susceptibilities ranging from 13 to 7112 × 10⁻⁶ SI (Fig. 2; Table 1). The smallest value corresponds to carbonate melt at 894.88 m. The other 20 (suevite) samples have an average of 2000 × 10⁻⁶ SI. These values are significantly higher than the average 55 × 10⁻⁶ SI reported from UNAM-5 and 7 for the clast-rich upper ejecta breccia (Urrutia-Fucugauchi et al. 1996a). Remanent magnetizations were measured for the same samples on a Schoenstedt DSM-1 spinner magnetometer. Values range from 0.003 to 4.6 A/m with an average of 0.1 A/m (Fig. 2; Table 1). The corresponding Koenigsberger (Q) ratios (remanent versus induced magnetization) vary from 0.35 to 34.7 with an average of 1.5. Inclinations were measured on samples with core orientation lines marked, but show no coherent direction. Even those samples with Q >5, where remanent magnetization

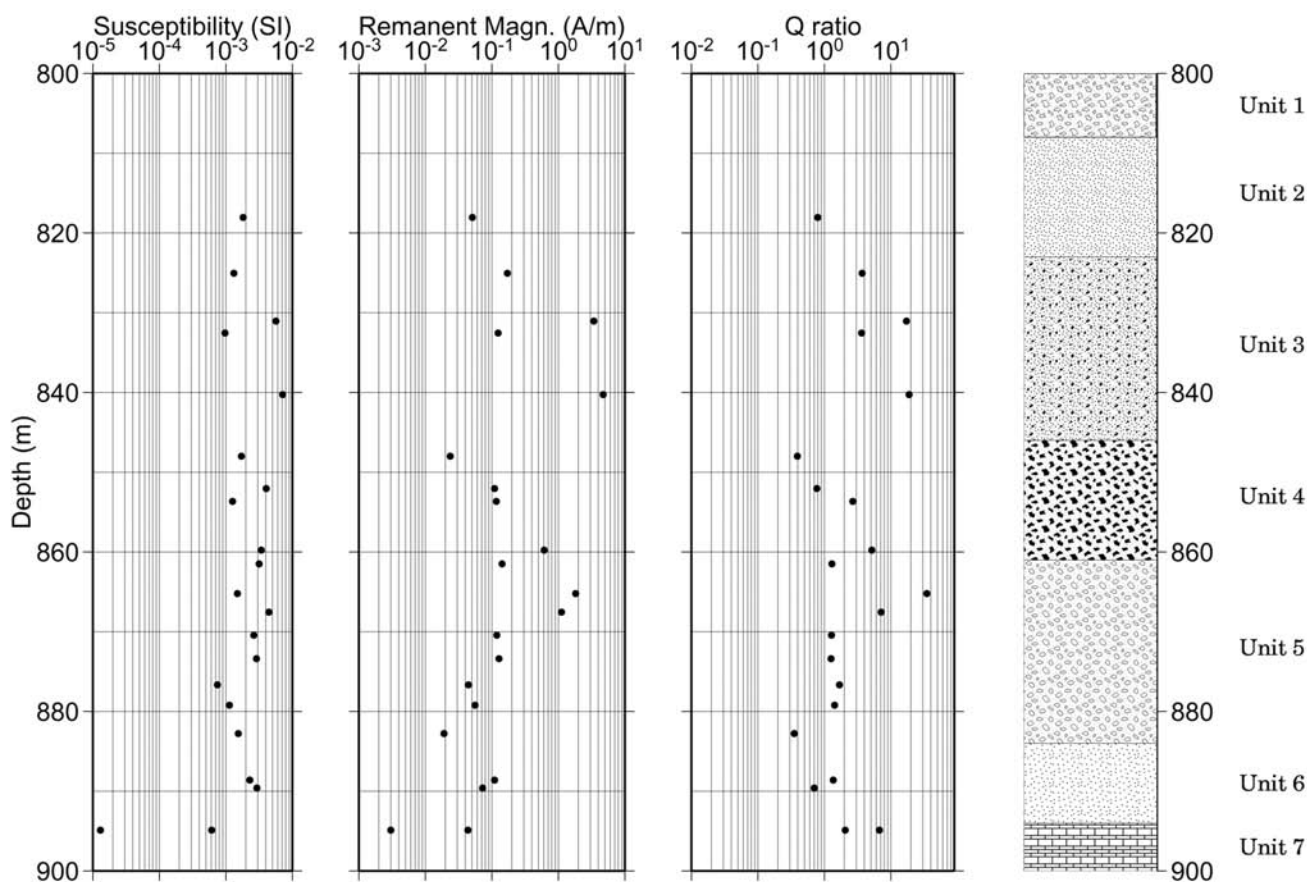


Fig. 2. Measured magnetic properties of Yax-1 core samples. Impactite unit stratigraphy is from Dressler et al. (2003) and has the following classification: unit 1 = redeposited suevite, unit 2 = suevite, unit 3 = melt-rich suevite, unit 4 = “heterogeneous suevite,” unit 5 = “brecciated suevite,” unit 6 = lower suevite, and unit 7 = limestone, dolomite, anhydrite.

Table 1. Magnetic properties of Yax-1 samples.

Depth ^a (m)	Susceptibility (SI × 10 ⁻⁶)	Remanent magnetization (A/m)	Koenigsberger ratio (Q)
818.05	1825	0.050851	0.79610
825.06	1326	0.17040	3.67162
831.03	5684	3.4293	17.2379
832.54	967	0.12361	3.65224
840.29	7112	4.6937	18.8563
848.02	1714	0.023611	0.39358
852.07	4068	0.110217	0.77410
853.66	1257	0.116899	2.65710
859.76	3416	0.61390	5.13466
861.51	3166	0.14277	1.28842
865.23	1499	1.82136	34.7157
867.57	4429	1.11087	7.16621
870.44	2650	0.11898	1.28280
873.39	2904	0.12781	1.25748
876.66	747	0.044374	1.69723
879.24	1123	0.055882	1.42175
882.78	1536	0.019007	0.35355
888.62	2299	0.109968	1.36666
889.63	2932	0.071952	0.70115
889.63f	45457	77.5	49.1876
894.88	13	0.003039	6.67978
894.91	610	0.043661	2.04501

^af denotes fragments.

predominates, show significant scatter with both normal and reversed directions.

No correlation between susceptibilities or remanent magnetizations and the suevite units of Stöffler et al. (2003) is apparent (Fig. 2). A single mafic basement clast (2.5 × 2.5 × 1.0 cm) was cut from the core at 889.63 m to determine a representative basement magnetization estimate to use in magnetic modeling. The clast has a remanent magnetization of 77 A/m, a susceptibility of 45457 × 10⁻⁶ SI, and a Q ratio of 49. These values are over an order of magnitude greater than normal crystalline basement levels (<5000 × 10⁻⁶ SI and <5 A/m, e.g., Clark 1997) and indicate enhanced magnetizations caused by some secondary process.

PETROGRAPHY OF FE-OXIDE PHASES

Fe-oxide phases comprising limonite-goethite, magnetite, and Fe-Ti-oxides are a common component of the impactite sequence in drillhole Yax-1 (Table 2). Orange, concentrically zoned, botryoidal limonite/goethite is abundant as an interstitial phase with coarse anhedral secondary calcite in the matrix of the reworked suevite, unit 1 (see Fig. 2 caption for unit definitions), at the top of the sequence (Fig. 3a). It occurs throughout the impactite sequence and as open space fillings in lithic basement fragments.

Magnetite, Fe-oxyhydroxides, and Fe-Ti-oxides are secondary minerals occurring in the groundmass to plagioclase and diopside microlites, vesicles associated with quartz and clay minerals, and veins associated with K-

feldspar and albite. Fine, 2–5 µm magnetite is commonly found in aggregates between plagioclase and diopside laths and may be concentrated at quartz and plagioclase lithic grain boundaries (Figs. 4a, b). Coarser 50–300 µm grains are commonly titaniferous (Fig. 4e). Vesicles may be lined with magnetite and filled with quartz and clay minerals (Figs. 3b, 3c, 3e, and 3f). Unit 3 (Fig. 2) contains highly vesicular to pumiceous silicate melt fragments with amygdalae infilled with fine-grained granular carbonate and secondary coarse carbonate. Fine spheroids of Fe-oxide line amygdalae and form rims on fragments (Figs. 3 and 4). The brown coloration of this unit is probably due to a combination of the fine grain size of the carbonate matrix, fine dusting of Fe-oxides within the melt fragments, and trace orange-reddish brown interstitial limonite (Figs. 3 and 4). The altered glass fragments in unit 4 are comparatively poor in vesicles and amygdalae relative to the units above that tend to host most of the Fe-oxides. Some fragments are stained orange brown possibly due to Fe-oxyhydroxides or dark chocolate brown due to ferrous iron. Fe-oxide spherules partially fill carbonate-saponite-quartz amygdalae (Figs. 3c–3f). The presence of magnetite-filled vesicles does not produce anomalously high susceptibility or remanent magnetization. Units 3, 5, and 6 contain abundant secondary Fe-oxides not only as vesicle fillings associated with quartz but also within the groundmass. The fine (<5 µm) dusting of Fe-oxides in the groundmass, in open spaces such as lithic–melt grain boundaries and amygdalae, is responsible for the higher susceptibilities and NRM levels within the impactites.

PETROGRAPHY OF MAGNETIC BASEMENT CLASTS

Mafic lithic fragments are a common component of the Yax-1 impactite sequence (ICDP 2002) and many are magnetic as indicated by a simple pen magnet. They range in size from ~0.5 to >2.5 cm, occurring as isolated fragments and as bomb cores (Fig. 5). Magnetization levels are partially a function of the size and abundance of the mafic basement fragments within the impactites. At 889.63 m (unit 6), a partial, 2.5 × 2.5 × 1 cm, metamorphic mafic basement clast produced the highest susceptibility and remanent magnetization (Figs. 5a, 6; Table 1). Unit 3 samples contain mafic metamorphic magnetic lithic clasts at 840.29 that also

form the nucleus for a simple cored bomb (Fig. 5b), and unit 5 samples also contain macroscopic <0.5 cm black magnetic fragments (Fig. 5c).

The basement lithology sampled by the impact consisted partially of metamorphosed gabbro to quartz gabbro. These metamorphic fragments consist of coarse boudinaged, opaque pseudomorphs possibly after pyroxene, quartz, feldspar, titanite, rutile, apatite, and zircon with interstitial spaces filled with montmorillonite, magnetite, quartz, and limonite. They are cut by veins of calcite and saponite. The <1.5 mm interstitial opaque pseudomorphs of amphibole (Fig. 6a) are replaced by 60–70% K-feldspar, 25–30% fine 1 μm ilmenite and titanomagnetite and ~5% stilpnomelane (Fig. 6b).

Table 2. Mineral compositions of Fe oxides in Yax-1.

Unit	1	1	2	3	5	5	5	6	6	6
Sample	806.41	806.41	818.05	831.02	862.25	862.25	862.25	882.78	882.78	882.78
Description	a	b	c	d	e	f	g	h	i	j
Mineral	Goethite-limonite	Goethite-limonite	Magnetite	Limonite	Magnetite	Magnetite	Magnetite	Magnetite	FeTi-oxide	FeTi-oxide
SiO ₂	5.61	4.29	0.24	4.56	5.82	3.91	5.18	2.99	4.05	5.72
TiO ₂	3.25	3.15	0.74	0.83	1.42	2.29	0.35	3.27	22.04	58.02
Al ₂ O ₃	3.30	2.98	0.05	2.62	2.34	1.42	2.00	1.13	1.13	1.45
Cr ₂ O ₃	0.00	0.00	0.05	0.00	0.00	0.00	0.00	0.09	0.02	0.00
FeO	52.45	52.82	89.76	67.32	80.46	82.38	82.62	83.74	49.91	25.16
MnO	0.20	0.25	0.09	0.12	0.10	0.12	0.01	0.03	0.00	0.08
NiO	0.01	0.10	0.02	0.01	0.07	0.00	0.05	0.01	0.00	0.09
MgO	1.30	1.13	0.06	0.28	1.06	0.28	0.10	0.02	0.16	0.22
CaO	0.59	0.52	0.04	0.27	0.18	0.25	0.25	0.12	2.12	1.93
BaO	0.01	0.05	0.03	0.00	0.00	0.13	0.07	0.05	0.54	0.56
Na ₂ O	0.15	0.24	0.00	0.16	0.25	0.15	0.21	0.16	0.28	0.30
K ₂ O	0.27	0.08	0.04	0.03	0.26	0.19	0.20	0.11	0.18	0.52
F	0.11	0.51	0.06	0.19	0.00	0.00	0.00	0.00	0.04	0.02
Cl	0.11	0.09	0.00	0.02	0.03	0.03	0.04	0.02	0.08	0.05
Total	67.37	66.21	91.18	76.40	91.99	91.15	91.10	91.74	80.55	94.13
Si	0.185	0.147	0.006	0.136	0.144	0.099	0.131	0.076	0.112	0.126
Ti	0.081	0.081	0.015	0.019	0.027	0.044	0.007	0.062	0.456	0.961
Al	0.128	0.120	0.002	0.092	0.068	0.043	0.060	0.034	0.037	0.038
Cr	0.000	0.000	0.001	0.000	0.000	0.000	0.000	0.002	0.000	0.000
Fe ³⁺	1.449	1.511	1.965	1.682	1.666	1.748	1.743	1.773	1.149	0.463
Mn	0.005	0.007	0.002	0.003	0.002	0.003	0.000	0.001	0.000	0.002
Ni	0.000	0.003	0.000	0.000	0.001	0.000	0.001	0.000	0.000	0.002
Mg	0.064	0.057	0.002	0.012	0.039	0.011	0.004	0.001	0.007	0.007
Ca	0.021	0.019	0.001	0.009	0.005	0.007	0.007	0.003	0.063	0.046
Ba	0.000	0.001	0.000	0.000	0.000	0.001	0.001	0.001	0.006	0.005
Na	0.010	0.016	0.000	0.009	0.012	0.007	0.010	0.008	0.015	0.013
K	0.012	0.004	0.001	0.001	0.008	0.006	0.006	0.004	0.006	0.015
Σ cations	1.956	1.966	1.996	1.963	1.972	1.968	1.969	1.963	1.850	1.676
Fe ₂ O ₃	58.276	58.685	99.719	74.791	89.394	91.525	91.794	93.036	55.446	27.948
Total	73.19	72.07	101.14	83.87	100.92	100.30	100.27	101.03	86.09	96.92

^aConcentrically zoned colloidal orange mineral.

^bConcentrically zoned colloidal orange mineral, darker rim.

^cSkeletal magnetite in fragment.

^dDark ring in amygdale filling.

^eOpagues in vein.

^fOpaque bleb in vein.

^gColloidal opagues lining amygdale.

^hSpongy botryoidal Fe-oxide in small amygdale in glass fragment.

ⁱFine-grained ilmenite in carbonate.

^jFine-grained FeTi-oxide interstitial to carbonate.

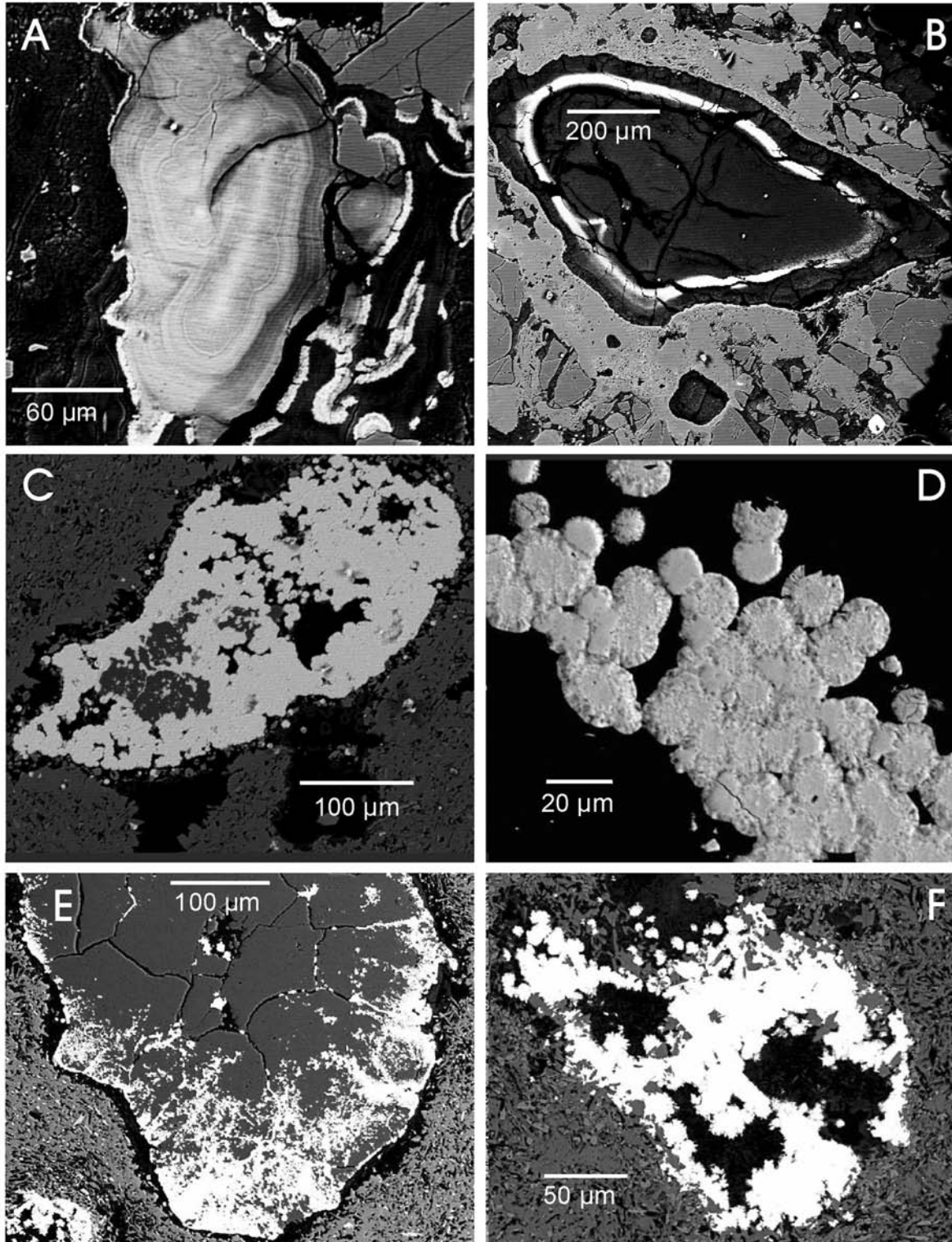


Fig. 3. Textural characteristics of Fe-oxides within the impactite samples, typically with low susceptibility and low remanent magnetization: a) concentric zoning, orange colloidal goethite interstitial to fragments, 806.41 m; b) magnetite occurs as lining of vesicle associated with clay minerals, 831.03 m; c) fine-grained aggregates of 10 μm magnetite associated with quartz filling vesicle in plagioclase/diopside matrix of melt fragment, 882.78 m; d) close up of 20 μm magnetite spheroids within vesicle filling in (c), 882.78 m; e) fine magnetite along outer edge of quartz-filled vesicle within melt fragment, 882.78 m; f) fine spheroidal magnetite (white) associated with K-feldspar euhedra (medium gray) and saponite (black) within vesicle, 882.78 m.

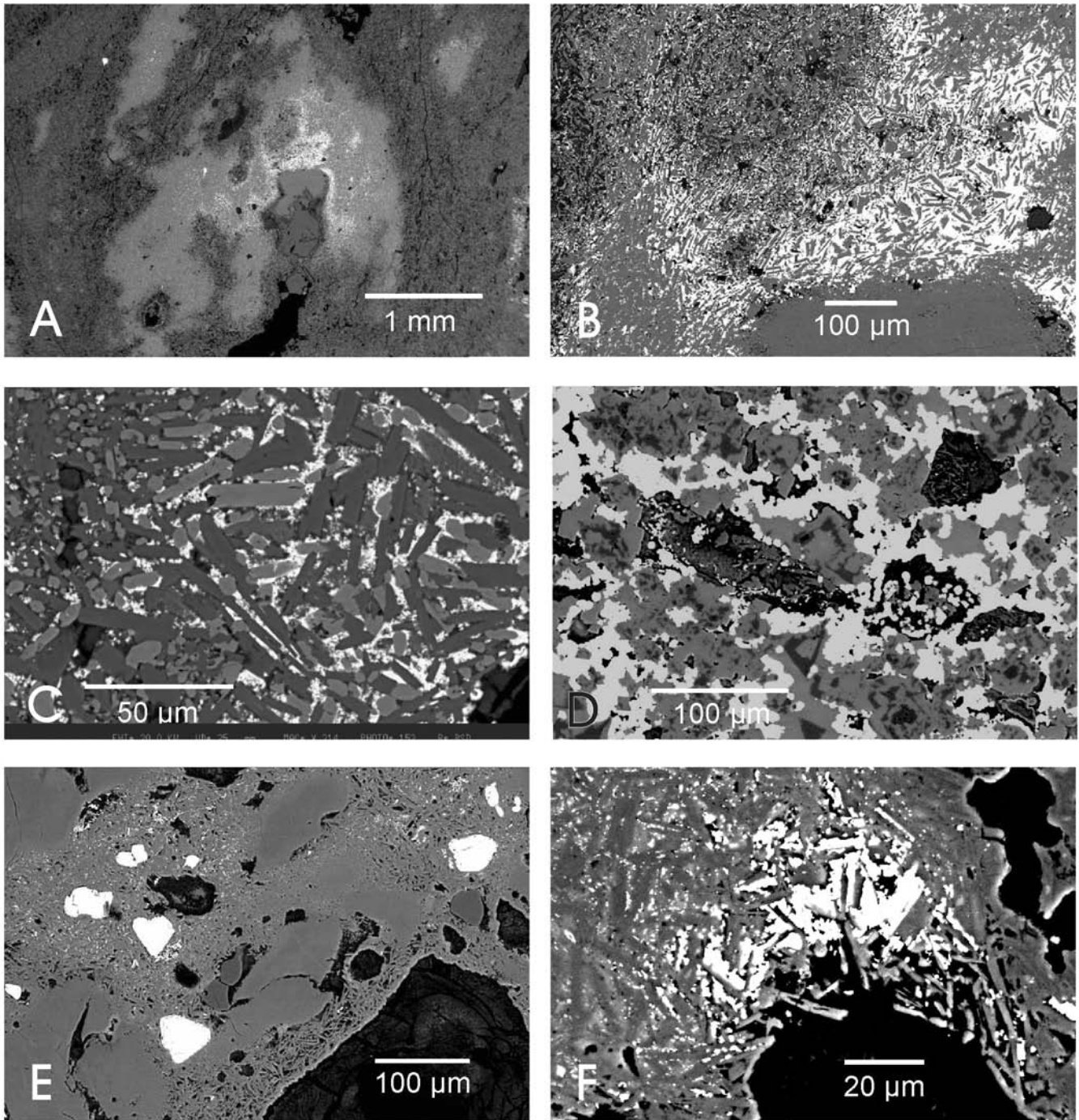


Fig. 4. Textural characteristics of the Fe-oxides within impactites with high susceptibility and high remanent magnetization, backscatter SEM images: a) magnetite (bright) associated with K-feldspar alteration concentrated around plagioclase (medium gray) and quartz (darker gray) lithic fragments, within silicate melt fragment, unit 5, 867.57 m; b) a close-up of (a). Secondary magnetite (<5 μm) forming the groundmass to plagioclase microlites (medium gray) and pyroxene laths (lighter gray left side of image). Bottom of image is plagioclase lithic fragment, 867.57 m; c) a close-up of silicate melt groundmass, 867.57 m. Melt composed of plagioclase laths (dark gray) and diopside laths and equant grains (medium gray) in groundmass of secondary magnetite (bright); d) matrix of impactite with large magnetic lithic fragment. Secondary carbonates (calcite medium gray, dolomite dark gray) and magnetite form the matrix to silicate melt fragments. Calcite-magnetite mineral association, 889.63m, unit 6; e) plagioclase lithic fragments and 20 to 40 μm subhedra of titaniferous magnetite within a matrix composed of plagioclase microlites, fine 5 μm grains of ilmenite, magnetite and trace rutile. Bottom right corner is large black clay altered fragment, 831.03 m, unit 3; f) aggregates of 2 to 5 μm magnetite grains form the matrix to plagioclase laths in silicate glass on the edge of dark clay filled vesicle, 831.03 m, unit 3.

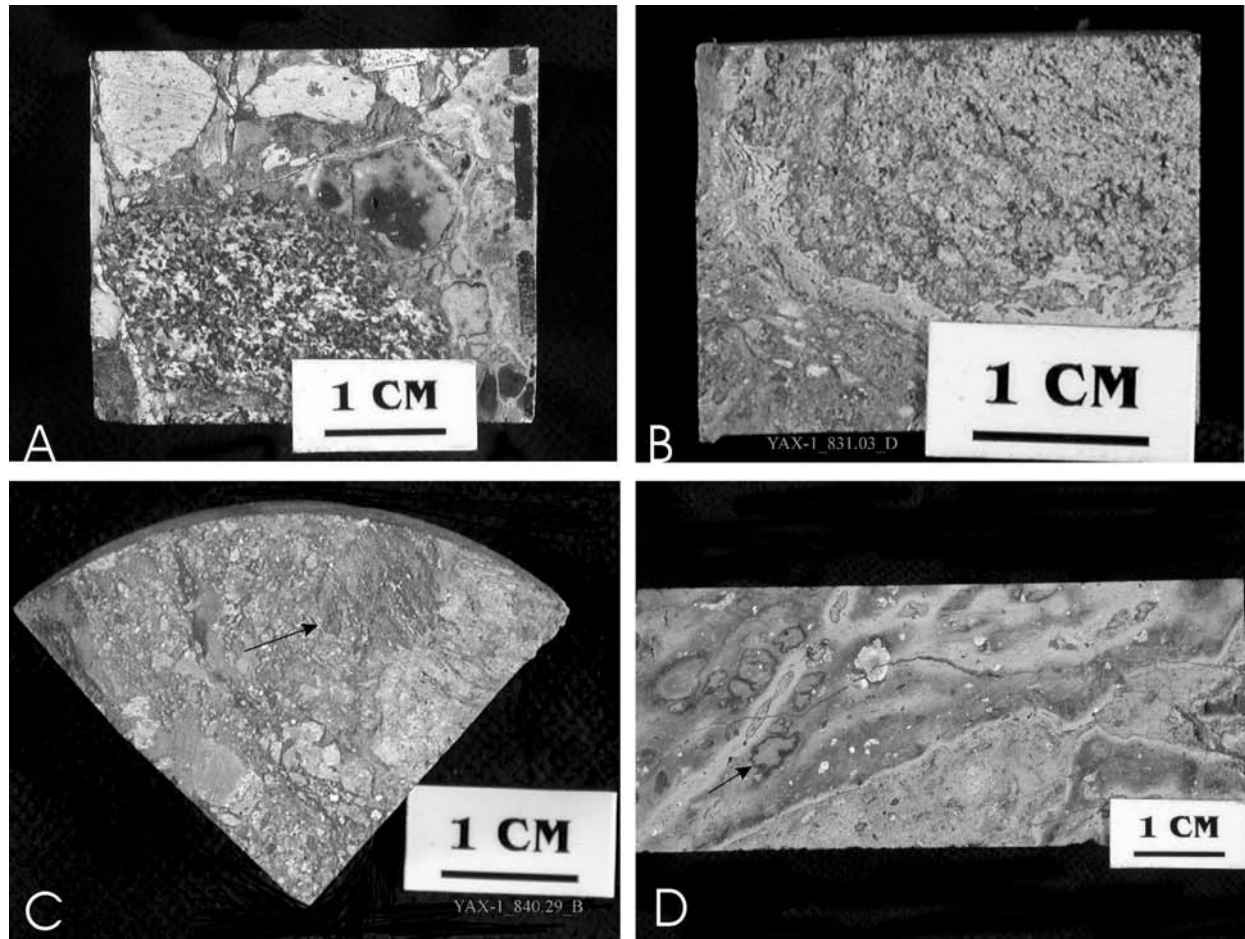


Fig. 5. Examples of magnetic basement fragments within the impactite sequence, Yax-1: a) intensely magnetic, metamorphosed quartz gabbro fragment in unit 6, at 889.63 m, $2.5 \times 2.5 \times 1$ cm; b) strongly magnetic metamorphic fragment, $2.5 \times 1.75 \times 1$ cm, in core of simple cored bomb, 831.03 m. Orange staining due to late secondary limonite; c) strongly magnetic mafic lithic fragment, 840.29 m, ~ 1 cm, common in unit 3; d) moderately magnetic impactite with fine secondary magnetite haloes on quartzite lithic fragments, weathers reddish brown, 867.57 m, unit 5.

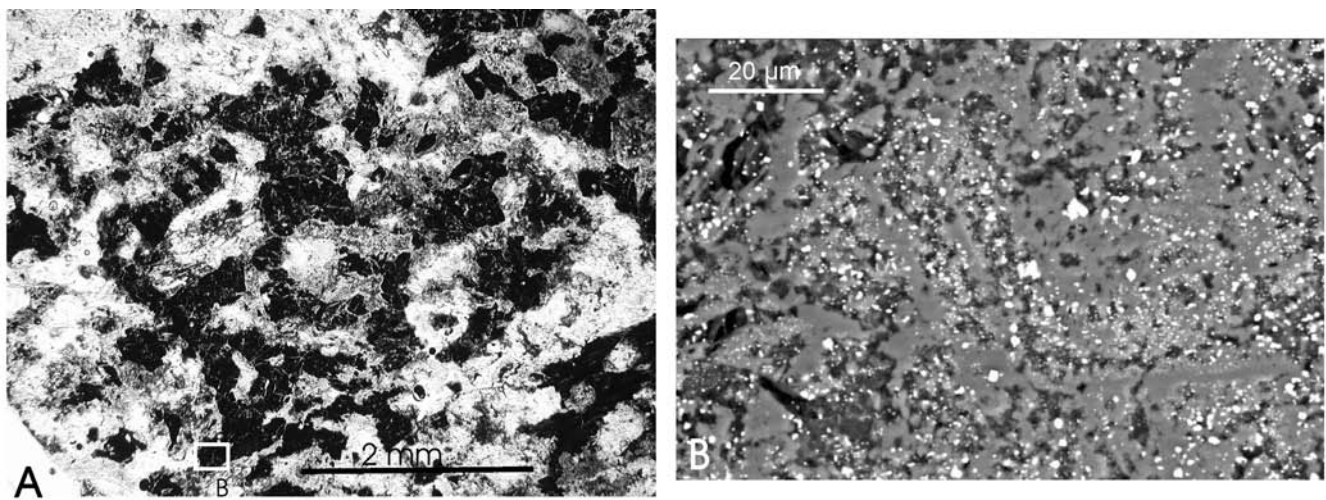


Fig. 6. Mineralogy and textures of strongly magnetic basement lithic fragments: a) 1–2 mm interstitial black opaque pseudomorphs after amphibole; b) backscatter photograph of inset shown in (a). Alteration consists of K-feldspar (medium grey), $\sim 1 \mu\text{m}$ ilmenite and titanomagnetite (white) with subordinate stilpnomelane (dark).

The Fe-oxide phases in the lithic fragments are secondary and similar to the secondary mineral assemblages described in the impactites (cf., Ames et al. 2004). However, the primary Fe-Mg minerals have been altered in the lithic fragments in contrast to the fresh unaltered diopside microlites in some of the impact melt. Hence, the intense magnetization produced by this type of alteration in the lithic fragments pre-dates the impact.

The relative intensities of magnetization within the impactite sequence are reflective of the size and abundance of: 1) altered quartz gabbroic basement fragments; 2) fine magnetite dusting ($\sim 3 \mu\text{m}$) forming the matrix of plagioclase/diopside microlites; and 3) fine magnetite as vesicle fillings. Strongly magnetized samples can have 1, 2, and 3 (e.g., large basement clast at 889.63 m), moderately magnetized samples have 2 and 3 (e.g., unit 3 samples at 831.03 and 840.29 m and small mafic fragments) and weakly magnetized samples have 3 only (e.g., at 882.78 m).

CONSEQUENCES FOR ANOMALY INTERPRETATION

Magnetic modeling shows that sources with a thickness and depth equal to the impactite series in Yax-1 (i.e., 800–900 m) and lateral dimensions of 1 km require magnetizations of $>1.5 \text{ A/m}$ to produce a 50 nT anomaly (the average size of anomalies outside the transient cavity at Chicxulub). This level of magnetization is somewhat higher than the range of measured values (0.08–0.60 A/m) for impact melt and melt breccia from Y-6 (Sharpton et al. 1992; Urrutia-Fucugauchi et al. 1994; Steiner 1996) and more than an order of magnitude greater than the Yax-1 sample average of 0.1 A/m. The latter would only produce a 3 nT anomaly assuming the same source dimensions. Indeed, the field over the vicinity of Yax-1 is very subdued, indicating that the Yax-1 average magnetization is representative of the immediate region (i.e., within a 10 km radius).

Limonite and goethite phases found within the Yax-1 impactite sequence are of little significance regarding anomalous magnetic effects, both having small susceptibilities and remanent magnetizations (e.g., Clark 1997). It is the Fe-Ti-oxides, especially the Ti-poor varieties such as magnetite, that are important in producing observable magnetic anomalies. Magnetite with grain sizes 0.01–20 μm is in the pseudo-single domain (PSD) range and can carry a stable and, possibly intense, natural remanent magnetization (NRM). It mimics the behavior of truly single-domain (SD) magnetite (grain size $<0.01 \mu\text{m}$) and is characterized by low susceptibilities and, hence, large Q values ($\gg 1$). Grains larger than 20 μm have a multi-domain (MD) state, in which susceptibilities are higher and NRMs lower leading to Q values usually $\ll 1$. Therefore, the relative volumes of SD, PSD, and MD magnetite control whether remanent magnetization or susceptibility is predominant in producing a

magnetic effect. An additional control is exerted by the direction of NRMs in a given volume. If the NRM directions of grains are scattered widely, then the resultant magnetic effect may be small, even though individual grains carry a large remanent magnetization component.

For the Yax-1 samples, magnetite occurring in vesicles associated with quartz and clay minerals is generally in the multi-domain size range ($>20 \mu\text{m}$; e.g., Fig. 3c–f). Smaller grain sizes ($<5 \mu\text{m}$) are associated with magnetite occurring in aggregates between plagioclase/diopside laths (Figs. 4c, f). For the sample at depth 882.78 m in unit 5, MD magnetite is dominant (Figs. 3c–3f) producing a small Q ratio of 0.35. At 831.03 m in unit 3, both MD (Fig. 4e) and PSD magnetite (Fig. 4f) are present in larger than average volumes giving high susceptibilities and NRM values (Table 1). The latter predominates, giving a high Q ratio of ~ 17 .

Within the mafic lithic fragments, alteration of Fe-Mg minerals is a major source of the magnetite present, which is mainly found in PSD sizes, usually $<3 \mu\text{m}$. In the fragment we have measured, the NRM and susceptibility are both very high but the PSD magnetite has a sufficient volume to predominate, giving a Q ratio of ~ 49 . Taking the mafic fragment magnetization of 77 A/m and assuming the melt matrix has a 0.5 A/m magnetization (representative of measured values), then with a unidirectional remanent magnetization direction, only a $\sim 6\%$ volume of mafic clast material is needed to produce a 5 A/m source (i.e., the modeled magnetization level of magnetic zones presumed within the melt). Even though this percentage is small, the volume of clasts within the melt sheet at Chicxulub is expected to be smaller for such a large structure due to the long cooling times for the melt, leading to assimilation of clasts and the proportionately high ratio of melt versus fragmented target material compared to smaller structures. The basement clast magnetization is also pre-impact, so magnetization vectors for all the clasts incorporated into the melt would not be aligned in a coherent direction, as is the case for the concentric magnetic zones in the melt sheet.

Nonetheless, the very high remanent magnetization seen in mafic basement clasts in Yax-1 suggests that this kind of target material could be an important source component of the magnetic anomalies and of the Chicxulub melt composition. Information on basement lithologies at Chicxulub has come mainly from clasts found in other holes drilled within and outside the crater. Clasts found in Y-6 are mainly granite gneisses with subordinate rock types such as metaquartzite and quartz-mica schist (Sharpton et al. 1992; Schuraytz et al. 1994). Clasts logged in the Yax-1 core are predominantly felsic with 67% being classed as granitic lithologies (ICDP 2002). However, the remainder comprise intermediate to mafic compositions such as granodiorite, diorite, amphibolite, and gabbro. Indirect evidence from older drill holes such as Y-6 and C-1 also point to a more mafic component present in the Yucatán basement. Kring and Boynton (1992) suggested

pyroxenite, amphibolite, or diabase as possible target rocks based on a petrological study of Y-6 melt rocks. Geochemical analyses of impact melts from C-1 and Y-6 show a more mafic composition than observed in clasts, and isotopic data also require an intermediate to mafic component present in the basement rocks (Kettrup et al. 2000). The metamorphosed, magnetic mafic basement fragments present in Yax-1 are an important component, along with granitoids and carbonates, of the target rocks at Chicxulub.

The exact nature of the highly magnetized zones that produce the anomalous magnetic field at Chicxulub remains unclear. Within the impactites, only those samples containing magnetic basement clasts (e.g., 831.03 and 840.29 m) have magnetizations (3.4 and 4.7 A/m, respectively) that are comparable to the level (5 A/m) for the inferred hydrothermal zones in the melt sheet. Mineralogical observations and geochemical studies indicate that the impactite sequence in Yax-1 has only been subjected to low temperature oceanic alteration in an oxidizing environment (Ames et al. 2004). In contrast to that reported by Zurcher and Kring (2003), chlorite was not found as a higher temperature hydrothermal alteration product in the impact sequence. However, rare chlorite was identified within a metamorphosed basement clast but is not related to impact-induced hydrothermal activity. Zeolites characteristic of slightly higher temperature formation (100–200 °C; Palmason et al. 1979) are not present in the drilled impactite sequence. Therefore, the assemblages of secondary minerals in Yax-1 that consist of clay minerals, celadonite, saponite, montmorillonite, opal, magnetite, limonite, goethite, K-feldspar, carbonate, and trace sulfides, formed at low (<150 °C) temperatures (Ames et al. 2004). These temperature levels are lower than any hydrothermal alteration mechanisms inferred to be present within the cooling melt sheet. It is possible that Yax-1 intersected a distal seawater recharge zone to a more proximal hydrothermal system developed in the center of the crater. Only direct sampling of one of the magnetized zones within the melt, as proposed for a future offshore drill-hole (Morgan et al. 2000), will provide conclusive information.

Acknowledgments—We thank ICDP and UNAM for making core samples available. Ken Buchan and Richard Ernst are thanked for their help in carrying out magnetic property measurements on the core as well as C. Venance, I. M. Kjarsgaard and P. Hunt for mineralogical assistance. This is Geological Survey of Canada contribution 2003222.

Editorial Handling—Dr. Jaime Urrutia-Fucugauchi

REFERENCES

- Alexopoulos J. S. and McKinnon W. B. 1994. Large impact craters and basins on Venus: Implications for ring mechanics on the terrestrial planets. In *Large meteorite impacts and planetary evolution*, edited by Dressler B. O., Grieve R. A. F., and Sharpton V. L. Special Paper 293. Boulder: Geological Society of America. pp. 29–50.
- Ames D. E., Kjarsgaard I. M., Pope K. O., Dressler B. O., and Pilkington M. 2004. Secondary alteration of the impactite and mineralization in the basal Tertiary sequence, Yaxcopoil-1, Chicxulub impact crater, Mexico. *Meteoritics & Planetary Science* 39:1145–1167.
- Clark D. A. 1997. Magnetic petrophysics and magnetic petrology: Aids to geological interpretation of magnetic surveys. *AGSO Journal of Australian Geology & Geophysics* 17:83–104.
- Dressler B., Sharpton V. L., Morgan J., Buffler R., Moran D., Smit J., Stöffler D., and Urrutia-Fucugauchi J. 2003. Investigating a 65 Ma-old smoking gun: Deep drilling of the Chicxulub impact structure. *Eos Transactions* 84:125–130.
- Espindola J. M., Mena M., de la Fuente M., and Campos-Enriquez J. O. 1995. A model of the Chicxulub impact structure (Yucatán, Mexico) based on its gravity and magnetic signatures. *Physics of the Earth and Planetary Interiors* 92:271–278.
- Hildebrand A. R., Penfield G. T., Kring D. A., Pilkington M., Camargo A., Jacobsen S. B., and Boynton W. V. 1991. Chicxulub crater: A possible Cretaceous-Tertiary boundary impact crater on the Yucatán peninsula, Mexico. *Geology* 19:867–871.
- Hildebrand A. R., Pilkington M., Connors M., Ortiz-Aleman C., and Chavez R. E. 1995. Size and structure of Chicxulub crater revealed by horizontal gravity gradients and cenotes. *Nature* 376: 415–417.
- International Continental Drilling Program (ICDP). 2002. *Log of Yax-1 core*. <http://www.icdp-online.de>.
- Kettrup B., Deutsch A., Ostermann M., and Agrinier P. 2000. Chicxulub impactites: Geochemical clues to the precursor rocks. *Meteoritics & Planetary Science* 35:1229–1238.
- Kring D. A. and Boynton W. V. 1992. Petrogenesis of an augite-bearing melt-rock in the Chicxulub structure and its relationship to K/T impact spherules in Haiti. *Nature* 358:141–144.
- Lopez-Ramos E. 1975. Geological summary of the Yucatán peninsula. In *The ocean basins and margins, vol. 3: The Gulf of Mexico and the Caribbean*, edited by Nairn A. E. M. and Stehli F. G. New York: Plenum Press. pp. 257–282.
- Morgan J., Buffler R., Urrutia-Fucugauchi J., and Grieve R. 2000. *Chicxulub: Drilling the K-T impact crater*. Ocean Drilling Program Full Drilling Proposal. p. 26.
- Palmason G., Arnorsson S., Fridleifsson I. B., Kristmannsdottir H., Saemundsson K., Stefanasson V., Steingrimsson B., Tomasson J., and Kristjansson O. 1979. The Iceland crust: Evidence from drillhole data on structure and processes. In *Deep drilling results in the Atlantic Ocean: Ocean crust*, edited by Talwani M., Harrison C. G., and Hayes D. E. Maurice Ewing Series, vol. 2. Washington D.C.: American Geophysical Union. pp. 43–65.
- Penfield G. T. and Camargo A. 1981. Definition of a major igneous zone in the central Yucatán platform with aeromagnetism and gravity (abstract). 51st Annual Meeting of the Society of Exploration Geophysicists. p. 37.
- Pilkington M., Hildebrand A. R., and Ortiz-Aleman C. 1994. Gravity and magnetic modelling and structure of the Chicxulub crater, Mexico. *Journal of Geophysical Research* 99:13147–13162.
- Pilkington M. and Hildebrand A. R. 2000. Three-dimensional magnetic imaging of the Chicxulub crater. *Journal of Geophysical Research* 105:23479–23491.
- Rebolledo-Vieyra M. 2001. Magnetostratigrafía y paleomagnetismo del cráter de impacto de Chicxulub, Ph.D. thesis, Universidad Nacional Autónoma de México, Mexico D.F., Mexico.
- Schuraytz B. C., Sharpton V. L., and Marin L. E. 1994. Petrology of impact-melt rocks at the Chicxulub multiring basin, Yucatán, Mexico. *Geology* 22:868–872.
- Sharpton V. L., Dalrymple G. B., Marin L. E., Ryder G., Schuraytz

- B. C., and Urrutia-Fucugauchi J. 1992. New links between the Chicxulub impact structure and the Cretaceous/Tertiary boundary. *Nature* 359:819–821.
- Steiner M. B. 1996. Implications of magneto-mineralogic characteristics of the Manson and Chicxulub impact rocks. In *The Cretaceous-Tertiary event and other catastrophes in Earth history*, edited by Ryder G., Fastovsky D., and Gartner S. Special Paper 307. Boulder: Geological Society of America, pp. 89–104.
- Stöffler D., Hecht L., Kenkmann T., Schmitt R.T., and Wittmann A. 2003. Properties, classification, and genetic interpretation of the allochthonous impact formations of the ICDP Chicxulub drill core Yax-1 (abstract #07237). *Geophysical Research Abstracts* 5.
- Urrutia-Fucugauchi J., Marin L., and Sharpton V. L. 1994. Reverse polarity magnetized melt rocks from the Cretaceous/Tertiary Chicxulub structure, Yucatán peninsula, Mexico. *Tectonophysics* 237:105–112.
- Urrutia-Fucugauchi J., Marin L., and Trejo-Garcia A. 1996a. Initial results of the UNAM scientific drilling program on the Chicxulub impact structure: Rock magnetic properties of UNAM-7 Tekax borehole. *Geofísica Internacional* 35:125–133.
- Urrutia-Fucugauchi J., Marin L., and Trejo-Garcia A. 1996b. UNAM scientific drilling program of Chicxulub impact structure: Evidence of a 300 kilometer crater diameter. *Geophysical Research Letters* 23:1565–1568.
- Zurcher L. and Kring D. A. 2003. Preliminary results on the post-impact hydrothermal alteration in the Yaxcopoil-1 hole, Chicxulub impact structure, Mexico (abstract #1735). 34th Lunar and Planetary Science Conference. CD-ROM.
-